# CHANGES IN THE RADIAL AND TANGENTIAL DISTRIBUTION OF RADAR REFLECTIVITY DURING TROPICAL CYCLONE LANDFALLS OVER THE UNITED STATES

153

Corene J. Matyas[1] *, Jingyin Tang[1], Stephanie Zick[2], Markus Schneider[1]
[1]University of Florida, Gainesville, Florida; [2]Virginia Tech, Blacksburg, Virginia

## 1. INTRODUCTION

The primary and secondary wind circulations in a tropical cyclone (TC) help to organize the spatial configuration of its rainbands. After landfall, the wind circulation weakens, decreasing convergence into the circulation center. Advection of relatively dry continental air masses can erode precipitation. Interaction with the middle latitude westerlies and associated troughs can lead to extratropical transition during which rainfall decreases on the equatorward side of the storm, but increases on the poleward side of the storm. All of these mechanisms should lead to less convection surrounding the circulation center, and less convection located near the circulation center.

This study employs Level II data from the Weather Surveillance Radar 1988 Doppler (WSR-88D) network to examine the changing spatial configurations of rainbands in TCs. We employ a new routine for the mosaicking of reflectivity data from multiple radars and convert values into polygons using a Geographic Information System (GIS). We calculate spatial metrics to represent the tangential and radial distribution of reflectivity values in accordance with the primary and secondary wind circulations within the storm.

As a TC moves over land, the storm's center should become increasingly exposed to the continental air mass, thereby decreasing the amount of reflectivity values around the circle and decreasing the closure metric. Reflectivity values should become more dispersed as rainfall decreases near the storm center. The rates of exposure and dispersion should differ according to whether the TC completes an extratropical transition or dissipates after landfall. In this case study, we profile changes in dispersion and closure for Hurricane Jeanne (2004), which eventually completed an extratropical transition while still within range of the WSR-88D network, and compare these patterns with those from Hurricane Humberto (2007), which dissipated after landfall.

* *Corresponding author address:* Corene J. Matyas, Univ. of Florida, Dept. of Geography, Gainesville, FL 32611-7315; e-mail matyas@ufl.edu

## 2. WSR-88D REFLECTIVITY PROCESSING

We select data from the WSR-88D network for our spatial analysis as they are available at a very high spatial and temporal resolution. Jeanne and Humberto occurred prior to the implementation of super resolution and dual-polarization, hence the spatial resolution is 1° by 1 km. A full scan of the atmosphere takes approximately 5-6 minutes. Both spatial metrics involve the position of the storm's circulation center in their calculation. However, the position of a TC's center is typically only available every 6 hours in HURDAT, and the precision is limited to 0.1°. Therefore, we perform a cubic spline interpolation of the storm positions from HURDAT to produce data every 5 minutes. We perform a visual inspection of these positions by overlaying them with the radar reflectivity data in a GIS and correct as necessary.

Now that the track positions are available, we utilize a map-reduce framework (Lakshmanan and Humphrey 2014) to process Level II reflectivity data from radars within 600 km of the storm center. As detailed in Tang and Matyas (2016), all inputs, intermediate results and outputs are represented as key-values pairs. This allows us to chain multiple map and reduce functions in a pipeline to operate on complex tasks in map-reduce jobs. The complete procedure includes four steps: preprocess, map function chain, reducing function chain and post-process.

After quality control and pre-processing, data are gridded at 3 km x 3 km x 0.5 km resolution every 5 minutes using data from a 10-minute moving window (Fig. 1). Values for grid cells with data from multiple radars are calculated using a time-distance weighted function (Lakshmanan et al. 2006). Cells with missing values are filled using a distance-weighted interpolation performed in a Geographic Information System (GIS) (Tang and

Matyas 2017). We extract data from an altitude of 3.5 km and draw contours that enclose regions of reflectivity that are greater than or equal to 25 dB*Z* to represent regions of lighter rainfall, and greater than or equal to 35 dB*Z* to represent regions of heavier rainfall that could contain convective cells Figure 2). We the convert the contours into polygons (Figure 3) before calculating the spatial metrics. A schematic diagram representing this process is available in Figure 4, which contains elements from Tang and Matyas (2016) and Tang and Matyas (2017).

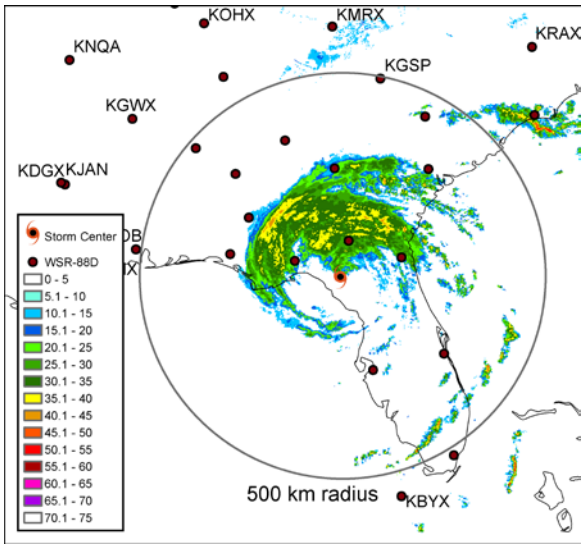


Fig. 1. Mosaicked Level II reflectivity data at 3.5 km altitude for Hurricane Jeanne (2004).

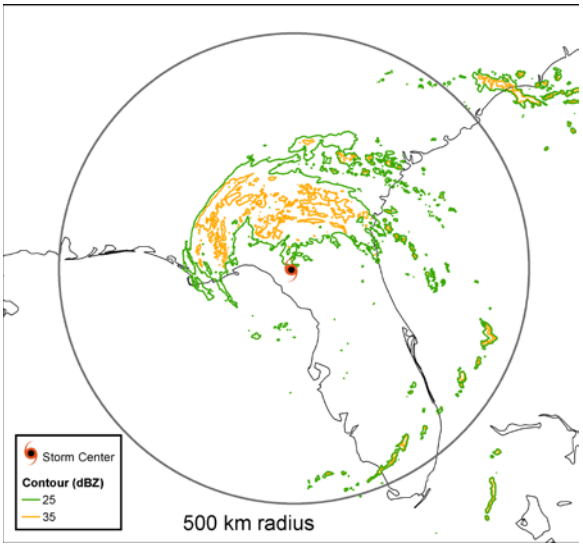


Fig 2. Contours enclosing regions of reflectivity ≥ 25 and 35 dB*Z* at the same time as in Figure 1.

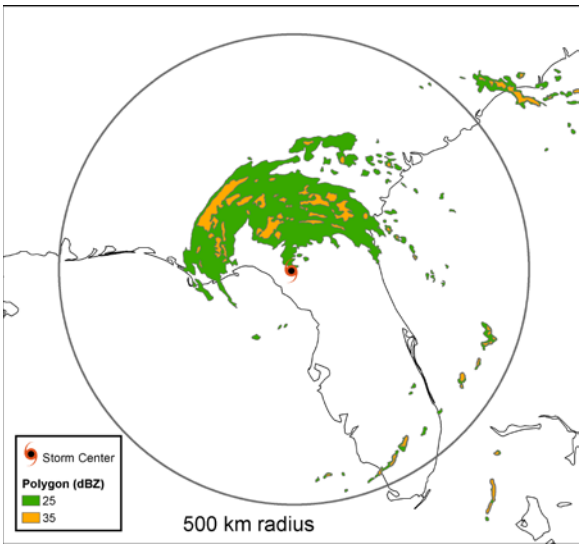


Fig. 3. Polygons representing regions of reflectivity ≥ 25 and 35 dB*Z* at the same time as in Figures 1 and 2.

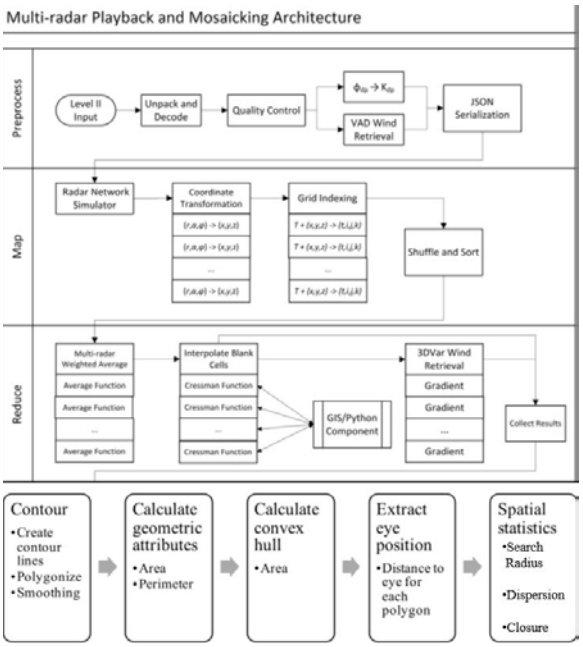


Fig. 4 Procedure to create multi-radar mosaic and spatial analysis in GIS.

## 3. SPATIAL METRIC CALCULATIONS

We consider the spatial distribution of reflectivity values by calculating measures of

their dispersion and closure. First, polygons smaller than 48 $km^2$ are removed from the analysis. For each remaining polygon, we calculate the center of mass and its distance from the TC's circulation center (Figure 5). Many studies employ a 500 km search radius (Larson et al. 2005; Villarini et al. 2014; Hernández-Ayala and Matyas 2016). For this reason, we employ a 500 km search radius and include all polygons that have their centroid within this radius.

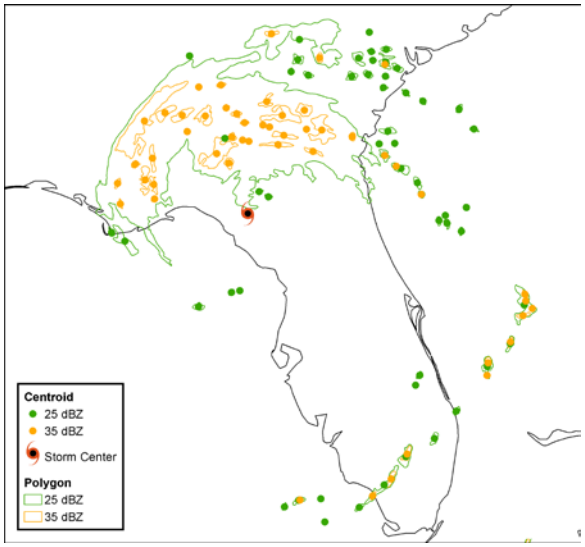


Fig. 5. Centers of mass for each polygon used in the calculation of the dispersion metric.

**Dispersion** (Equation 1) measures the radial distribution of precipitation with respect to the circulation center. This metric increases to a value of unity as the reflectivity region centroid(s) ($r_{centroid}$) move radially away from the circulation center toward the search radius ($r_{search}$) of 500 km. Each reflectivity region is weighted by its area, with larger regions receiving more weight, and the final metric is calculated by summing over all distinct reflectivity regions, with NP representing the number of polygons (Zick and Matyas 2016). Because Jeanne (2004) completed an extratropical transition, we expect it to lose convection within its inner core and its rain fields to expand poleward of the storm center, a process that is well-documented in the literature (Harr and Elsberry 2000; Klein et al. 2000; Jones et al. 2003; Matyas 2008; Zick and Matyas 2016). Thus dispersion should increase throughout the analysis period. Humberto experienced rapid intensification prior to landfall, thus its shape should become more compressed, meaning a decrease in dispersion during this period (Zick and Matyas 2016). However, entrainment of the relatively dry continental air mass should reduce convection near the storm's center which would cause dispersion to increase.

$$D = \frac{\sum_{i=1}^{NP} \frac{Area_i}{\sum_{j}^{NP} Area_j} \left( \frac{r_{centroid,i}}{r_{search}} \right)}{} \quad (1)$$

**Closure** (Equation 2) should decrease after landfall due to dry air entrainment regardless of whether or not the TC transitioned into an extratropical cyclone. As TC rainbands tend to curve, we quantify the degree to which the storm center is enclosed by reflectivity values (Matyas 2007; Matyas and Tang 2015). We count the number of 1° radials (Figure 6) emanating from the circulation center out to 500 km that intersect with a polygon (Figure 7) and divide by 360 so that a result of 1 indicates complete closure, while 0.5 indicates that only half of the arc around the TC is filled with reflectivity values.

$$C = \frac{no.\ 1°\ angles\ intersecting\ polygons}{360} \quad (2)$$

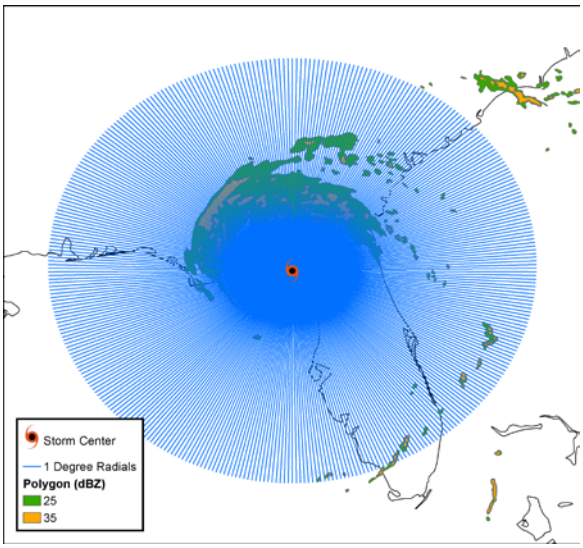


Fig. 6. Radials spaced each 1° outward from the TC's circulation center.

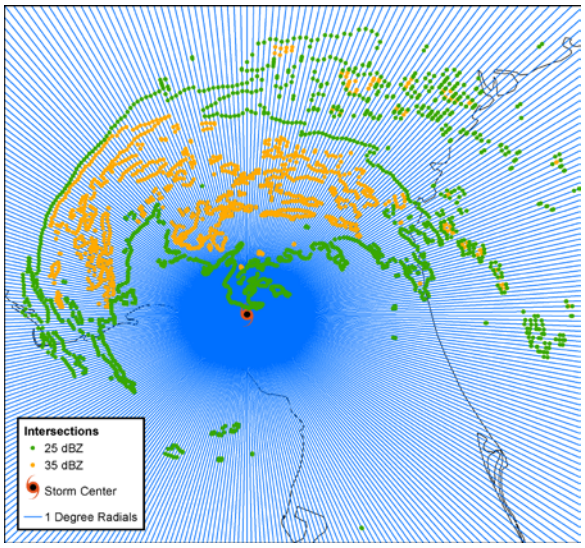


Fig. 7. Intersection of radials with polygon edges to calculate the closure metric.

## 4. RESULTS

According to Franklin et al. (2006), Hurricane Jeanne made landfall as a major hurricane over eastern Florida at 0400 UTC 26 September 2004. It weakened gradually to a tropical storm 14 hours after landfall, and then to a tropical depression 38 hours after landfall. It maintained a well-defined rain shield on its poleward side while moving northward and interacting with a frontal zone. It was declared post-tropical at 0000 UTC on 29 September. Our analysis window spans 0345 UTC 26 September - 2304 UTC 28 September (Figure 8).

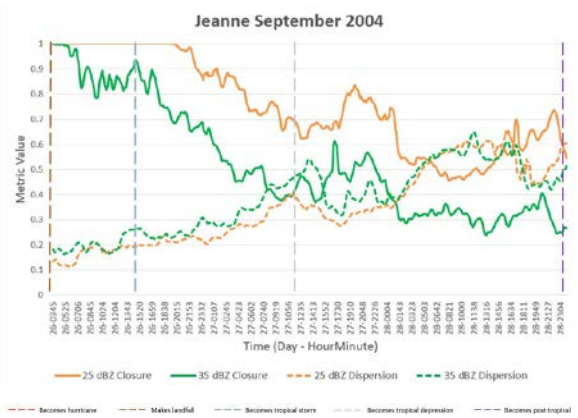


Fig. 8. Time series of metric values for Jeanne.

For Jeanne, dispersion increased linearly from landfall as rainfall decreased in the core until reaching TD intensity. Then rainfall became more linearly-orientated along a frontal boundary north of center around 1500 UTC 27 September. The rates of increase were 0.2 over 27 hours for 25 and 0.35 over 34 hours for 35 dB*Z*. Dispersion decreased briefly on the 27th due to development of a rainband 140 km east of center. Dispersion then increased more sharply (0.22 in 9.5 hours) as the core eroded and the main region of convection developed 200 km northeast of center, then levelled off as rainfall again stretched linearly north of center along the frontal zone and spine of the Appalachian Mountains.

In terms of the closure metric, 35 dB*Z* closure began to markedly and consistently decrease when Jeanne weakened to a TS and this trend in 25 dB*Z* began 5 hours later. Closure decreased over a 15-hour period at a rate of 7°per hour. Although the inner core continued to be exposed, a 7 (11) hour increase in closure occurred due to development of an outer rainband 400 km east of center on 27 September. Closure increased for 25 dB*Z* as Jeanne merged with a frontal system and became extratropical. The increase was due to a rainband 300 km east of center that lengthened towards the south. As this band did not contain large regions of convective cells, only a slight increase in closure is observed in the 35 dBZ regions at this time.

Humberto's development differed quite markedly from that of Jeanne in the hours prior to landfall. Humberto formed close to land and rapidly intensified from a tropical depression into a hurricane before landfall at 0700 UTC 13 September 2007 as a Category 1 Hurricane (Brennan et al. 2009). Humberto also spent less time over land compared to Jeanne, becoming a tropical depression by 0000 UTC 14 September and dissipating 18 hours later. Our analysis window spans 1900 UTC 12 September - 1152 UTC 14 September.

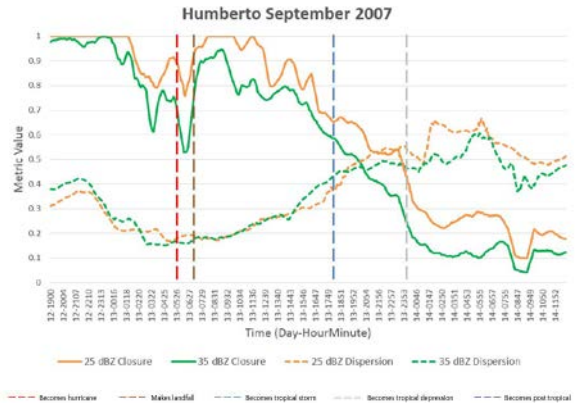


Fig. 9. Time series of metric values for Humberto.

Humberto formed close to shore and was intensifying at the time of landfall, which explains the rapid changes in shape that occurred early on 13 September. Rainfall was located mainly east of center while the core developed, leading to an exposed center where closure values fell from 0.8 to 0.6 for 25 dB*Z* regions. Rainfall became more centralized as hurricane intensity was achieved with decreasing values of dispersion occurring during this period. After landfall, closure decreased by 19° per hour for 12.5 hours, leveling off after weakening to a tropical depression. Rainfall remained east of center during the entire analysis period. After landfall, rainfall became more dispersed at a rate of 0.3 over 14 hours, again leveling off after weakening to a tropical depression and with little rainfall remaining in the core. The decreasing trend in closure also levelled off around the time that Humberto weakened to a tropical depression.

## 5. CONCLUSIONS AND FUTURE WORK

This study examined changes in the radial and tangential distribution of radar reflectivity regions in two landfalling hurricanes. We created a 3D mosaic of reflectivity data from the WSR-88D network and extracted values along a constant altitude of 3.5 km. At 5-minute intervals, we used a GIS to calculate dispersion, or the spread of reflectivity regions outwards from the storm center, and closure, or the tangential completeness of reflectivity surrounding the circulation center. We employed a search radius of 500 km and included all polygons whose centroids fell within this radius. We compare results for Hurricane Jeanne (2004), which spent more than two days over land and interacted with a frontal boundary before transitioning into an extratropical cyclone, and Hurricane Humberto (2007), which rapidly intensified prior to landfall and then dissipated within two days.

We find that despite the differences in storm histories, changes in the trend of dispersion and closure occur in conjunction with changes in storm intensity. Although the slopes are greater for Humberto than for Jeanne, trends in both metrics level off when each TC weakens to a tropical depression. Dispersion increased from 0.2 to 0.6 in both TCs, but took 48 (24) hours for Jeanne (Humberto). Closure in Jeanne (Humberto) decreased by 50 (85) % in 35 (24) hours. Jeanne's interaction with a frontal boundary and topography coincided with brief re-organization. In contrast, Humberto's increases (decreases) in dispersion (closure) occur at constant rate until weakening to TD. Correlation coefficients between dispersion and closure averaged -0.87.

Future work will examine changes in environmental conditions and their associations with shape change. We will extract data pertaining to vertical wind shear and total precipitable water from the NCEP Global Forecasting System (GFS) model analyses to calculate how these conditions changed over time. We will also examine the spatial patterns of moisture utilizing methods similar to Matyas (2017) to trace the advection of dry air into the core of the storm. We are also currently utilizing dispersion and closure along with three other metrics to compare radar observations with 6 simulations of the Weather Research and Forecasting model during the landfall of Hurricane Isabel (2003) (Matyas et al. 2017).

## 6. ACKNOWLEDGEMENTS

This research was funded through the University of Florida Research Opportunity Fund and a CAREER Award from the National Science Foundation (BCS 1053864).

## 7. REFERENCES


Brennan, M. J., R. D. Knabb, M. Mainelli, and T. B. Kimberlain, 2009: Atlantic hurricane season of 2007. *Mon. Wea. Rev.*, **137,** 4061-4088.

Franklin, J. L., R. J. Pasch, L. A. Avila, J. L. Beven, M. B. Lawrence, S. R. Stewart, and E. S. Blake, 2006: Atlantic hurricane season of 2004. *Mon. Wea. Rev.*, **134,** 981-1025.

Harr, P. A., and R. L. Elsberry, 2000: Extratropical transition of tropical cyclones over the western North Pacific. Part I: Evolution of structural characteristics during the transition process. *Mon. Wea. Rev.*, **128,** 2613-2633.

Hernández-Ayala, J. J., and C. J. Matyas, 2016: Tropical cyclone rainfall over Puerto Rico and its relations to environmental and storm specific factors. *Int. J. Climatol.*, **36,** 2223-2237.

Jones, S. C., and Coauthors, 2003: The extratropical transition of tropical cyclones: Forecast challenges, current understanding, and future directions. *Wea. Forecasting*, **18,** 1052-1092.

Klein, P. M., P. A. Harr, and R. L. Elsberry, 2000: Extratropical transition of western North Pacific tropical cyclones: An overview and conceptual model of the transformation stage. *Wea. Forecasting*, **15,** 373-395.

Lakshmanan, V., and T. W. Humphrey, 2014: A MapReduce technique to mosaic continental-scale weather radar data in real-time. *IEEE Journal of Selected Topics in Applied Earth Observations and Remote Sensing*, **7,** 721-732.

Lakshmanan, V., T. Smith, K. Hondl, G. J. Stumpf, and A. Witt, 2006: A real-time, three-dimensional, rapidly updating, heterogeneous radar merger technique for reflectivity, velocity, and derived products. *Wea. Forecasting*, **21,** 802-823.

Larson, J., Y. P. Zhou, and R. W. Higgins, 2005: Characteristics of landfalling tropical cyclones in the United States and Mexico: Climatology and interannual variability. *J. Climate*, **18,** 1247-1262.

Matyas, C. J., 2007: Quantifying the shapes of US landfalling tropical cyclone rain shields. *Prof. Geogr.*, **59,** 158-172.

Matyas, C. J., 2008: Shape measures of rain shields as indicators of changing environmental conditions in a landfalling tropical storm. *Meteorological Applications*, **15,** 259-271.

Matyas, C. J., 2017: Comparing the spatial patterns of rainfall and atmospheric moisture among tropical cyclones having a track similar to Hurricane Irene (2011). *Atmosphere*, **8,** 165-185.

Matyas, C. J., and J. Tang, 2015: Measuring gaps in tropical cyclone rainbands using Level II radar reflectivity data. *69th Annual Interdepartmental Hurricanes Conference*, Jacksonville, FL.

Matyas, C. J., S. E. Zick, and J. Tang, 2017: Using spatial metrics to compare observed and simulated reflectivity during the landfall of Hurricane Isabel (2003). *Monthly Weather Review*, **In revision**

Tang, J., and C. J. Matyas, 2016: Fast playback framework for analysis of ground-based Doppler radar observations using Map-Reduce technology. *Journal of Atmospheric and Oceanic Technology*, **33,** 621-634.

Tang, J., and C. J. Matyas, 2017: Arc4nix: A cross-platform geospatial analytical library for cluster and cloud computing. *Computers & Geosciences*, **Under revision**

Villarini, G., R. Goska, J. A. Smith, and G. A. Vecchi, 2014: North Atlantic tropical cyclones and U.S. flooding. *Bull. Amer. Meteor. Soc.*, **95,** 1381-1388.

Zick, S. E., and C. J. Matyas, 2016: A shape metric methodology for studying the evolving geometries of synoptic-scale precipitation patterns in tropical cyclones. *Annals of the Association of American Geographers*, **106,** 1217-1235.